# Rotary Kiln Cylinder Deformation Measurement and Feature Extraction Based on EMD Method

Kai Zheng, Yun Zhang, Chen Zhao and Lei Liu

*Abstract*-- **Rotary kiln is a large key rotating machine for production in cement, chemical and metallurgical industries. It is important to measure the straightness deviation and surface deformation of kiln cylinder as they are important physical parameters for evaluating the operation state of the kiln. A new method for extracting the profile features from the collected data based on EMD algorithm was proposed. A filtering criterion using energy percentage of IMF components and correlation coefficient method was proposed in order to eliminate the pseudo IMF components. And the physical meaning of the effective IMF components was explained. We compared the proposed method with the traditional geometry method. The experimental results indicated that the proposed method is effective in extracting the features of the straightness deviation and the surface deformation of rotary kiln cylinder. Furthermore, it can not only be used to process the non-stationary and non-linear signals collected but also be used to eliminate the noise signal. Therefore, it can be taken as a new method for evaluating the operation state of rotary kiln.**

*Index Terms*— **Rotary kiln, deformation measurement, features extraction, empirical mode decomposition**

## I. Introduction

Rotary kiln is a key rotating machine for production in cement, chemical and metallurgical industries, featuring low speed and heavy load when running [1]–[3]. It is mainly composed of rotary kiln's cylinder, tyre, supporting rollers and piers, as shown in Fig.1 [2]. Maintaining 24-hour normal and reliable operation of a rotary kiln is very important for industrial production. And it is of great theoretical and engineering significance to evaluate its operation state.

Cylinder is a core subsystem of the rotary kiln supported by rollers. The straightness deviation and surface deformation of the rotary kiln cylinder are two important physical parameters used to evaluate the operation state of a rotary kiln [1]–[2]. Straightness deviation of a rotary kiln cylinder can reflect the dynamic changes in load bearing of supporting rollers [5]. Excessive load bearing can easily give rise to catastrophe fault of the rotary kiln [4]–[7]. And the surface deformation of the rotary kiln cylinder has an important influence on the working life of the lining bricks in the kiln [2]. The deformation of the kiln cylinder was composed of straightness deviation and surface deformation. And a key problem is to correctly extract the two components from the signals collected in order to evaluate the operation state of the kiln [1]. Most researchers obtained the two components by setting up a geometrical model. In [8], authors presented a method for measuring the straightness deviation and surface deformation of the rotary kiln cylinder, and preliminarily put forward the geometry methods for calculating the straightness deviation. In [1], researchers elaborated the significance of measuring the straightness deviation and surface deformation of a rotary kiln cylinder, and introduced a geometry method for the dynamic measurement of the kiln straightness deviation. However, due to the complex working conditions in the industrial field, there is low frequency vibration which affects the measurement process. Therefore, the actual measurement signals contained multiple information such as the straightness deviation, the surface deformation and the noise interference signals. And the traditional geometry method could only provide the geometry information of the signals, but could not make a comprehensive response to them. Moreover, most of times, the signals collected in the real industry field were non-stationary and non-linear signals, and it is not appropriate to process the signals by the traditional geometry method.

As a new signal processing method, empirical mode decomposition (EMD) method can analyze non-linear and non-stationary signals and achieve self-adaptive decomposition. It is free from selection of basis function and Heisenberg uncertainty principle [9]–[12]. In actual calculation, the empirical mode of signals can be obtained based on EMD decomposition and the phase function of signals can be acquired based on Hilbert transform. Then, the derivative of the phase function is calculated to get the instantaneous frequency of signals. Local properties of the instantaneous frequency can be used to accurately reflect local signal features. Therefore, EMD method can make up for the demerits of traditional signal analysis method [13]–[15]. It is superior over traditional method of time-frequency analysis of signals and can be used to extract features. Guo Qiang. et. al. combined EMD and chaos detection to extract the frequency slippage signal in

Manuscript received on May 02, 2015; this work was supported by the National centre for rotary kiln detection technology and Hubei Digital Manufacturing Key Laboratory in China.

Kai Zheng is with the School of Mechanical and Electronic Engineering, Wuhan University of Technology, Wuhan, China. Phone: +008615872410576; e-mail:zhengkai2001@163.com

Yun Zhang is with the School of Mechanical and Electronic Engineering, Wuhan University of Technology, Wuhan, China (corresponding author to provide phone: +008613871445062; e-mail: whkasco@aliyun.com).

Chen Zhao is with the School of Mechanical and Electronic Engineering, Wuhan University of Technology, Wuhan, China.

Lei Liu is with the School of Mechanical and Electronic Engineering, Wuhan University of Technology, Wuhan, China.

dense and complex full-pulse sequences [16]. Xia Chunlin et. al. studied the characteristics of engineering surfaces，and proposed the feature extraction method based on the Hilbert-Huang transform (HHT) and EMD method. And the new technique proposed is useful and complementary to other existing techniques [17]. Peng Yonghong investigated the effectiveness of a new time-frequency analysis method based on EMD and Hilbert transform for analyzing the no-stationary cutting force signal of the machining process [18]. Jose Antonino-Daviu. et. al. presented an EMD-based invariant feature extraction algorithm for rotor bar condition monitoring [19]. Fan Xianfeng et. al. employed empirical mode decomposition (EMD) to decompose raw vibration signals and extract the fault feature of the machine. The results indicated that the proposed method has superior capability to extract machine fault features from vibration signals [20].

In this paper, we presented an initial investigation on the EMD-based method for feature extraction of the kiln cylinder's profile, and analysis of the signals collected by the measurement system based on the proposed method and discussed the physical meanings of the IMF components. Finally, we compared the processed results with the traditional geometry method and made conclusions at the end of this paper.

This paper is organized as follows: Section II puts forward the measurement method and system; Section III and Section IV introduce geometry method and EMD method; Section V processes the signals collected according to the proposed method and compares it with the geometry method; Section VI makes several conclusions.

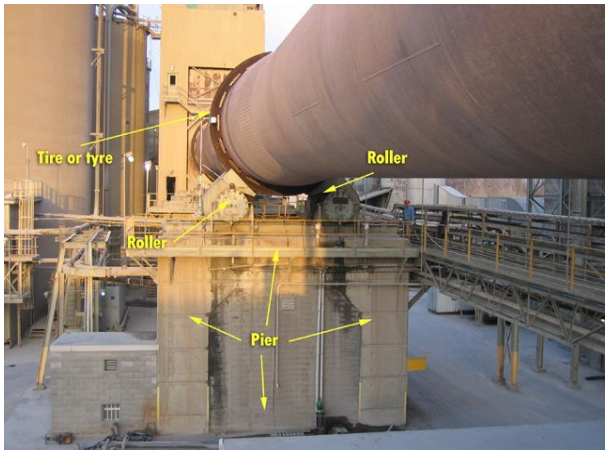


Fig.1. The physical map of a rotary kiln.

## II. Measurement Methods

The rotary kiln's cylinder consists of many linked cross sections. In practice, we measured the profile of each section. Based on the measurement results concerning all the sections, the straightness deviation of the rotary kiln cylinder and the surface deformation could be calculated. The measurement principle diagram is shown in Fig.2.

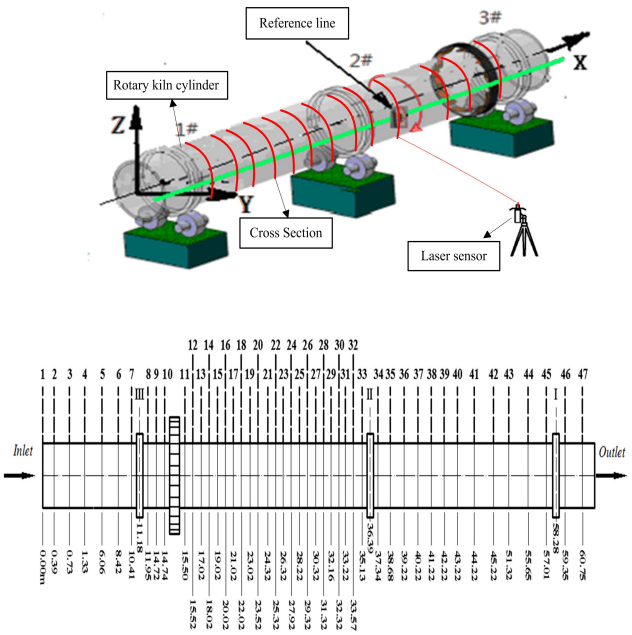


Fig.2. The diagram of the measurement principle

During the measurement, a number of cross sections (usually 30) were selected according to the length of the kiln and the starting measuring point on each section was chosen firstly. It requests that the starting measurement point on the cylinder of kiln should be in the same reference line, as shown in Fig.2. Under the influence of such factors as temperature and gravity, the cylinder of the kiln is deformed. And the sections of the cylinder are generally not round circle and have eccentricity and local deformation. Fig.3 (a) is a schematic diagram of measuring the section deformation of the rotating cylinder based on laser scanning. When the rotary kiln is rotating, the scanning spots $i(i=1,2,3,.....n)$ on the outer contour of the cylinder's cross section are moving in a circle with the centre of rotation as the centre of the circle. With the distances between the centre of the rotation and the spots $i$ as the radiuses, circles with different radiuses are formed. When the cylinder rotates once, what the measuring instrument acquires are different distances from the instrument to various spots $i$ on the cylinder surface: that is, $L_i$ and azimuth $\theta_i(\theta_i = 2\pi/n*i)$ .

Where $n$ is the number of points collected by laser sensor and can be calculated by the formula $n = f \cdot t$ . $f$ is the sample frequency and $t$ is the sample time. The measurement method is shown in Fig.3.

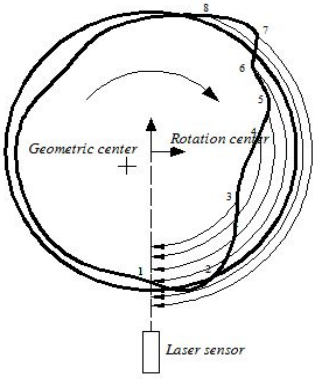


(a)

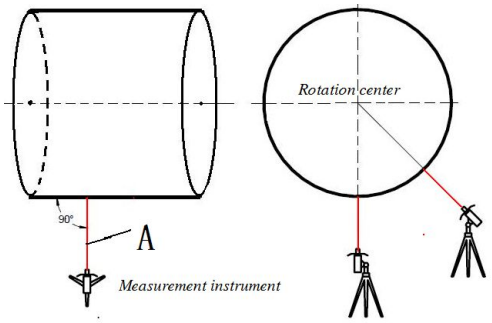


(b)

Fig.3 Diagram of the measurement method (a) Schematic diagram of measuring the section deformation of the rotating cylinder based on laser scanning (b) Diagram of the installation of the measurement instrument.

## III. Geometry Method

As mentioned in section II, the cylinder of the kiln is divided into N sections (N>20) along with coordinate X during the measurement. Then we measure the cross sections one after another using the laser sensor. The rotation straight line is surrounded by all of the measured sections while the rotary kiln rotates and the axis of the rotary kiln is the curve including all the geometric centres of the sections. The problem concerning the straightness deviation of the rotary kiln can be transformed into solving the geometric centre and the eccentricity of the measured sections. We assume that the radial deviation $\xi$ is the difference value between contours and base circle satisfied to restrain of:

$$\sum_{i=1}^{n}\zeta_i = 0, \sum_{i=1}^{n}\zeta_i^2 = \min \tag{1}$$

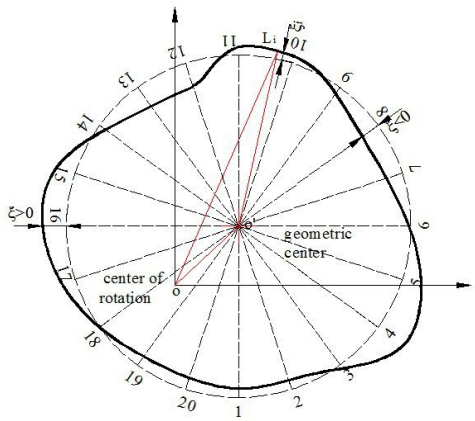


Fig.4 The geometrical model of the calculation method

As shown in Fig.4, there is an average circle of section profile, which is a base circle. By using the calculation method, the base circle based on the measured data can be calculated. The definitions of the parameters are as follows (Fig.4): $O$ is the rotation centre of the section; $O'$ is the geometric centre of the section and its coordinate is $(a,b)$; $L_i$ ( $x_i, y_i$ ) is the coordinate of the measured point $(i=1,2,.....n)$; $n$ is the number of measured points; R is the radius of the base circle; $r_i$ is the radius from point $L_i$ to the rotation centre of the section; the eccentricity is

$$e = \sqrt{a^2 + b^2} \tag{2}$$

By geometrical analysis of $\Delta L_i O O'$

$$r_i = e\cos(\theta_i - \varphi) + \sqrt{(R+\xi_i)^2 - [e\sin(\theta_i - \varphi)]^2} \tag{3}$$

As $e \ll R$ , $\sin(\theta_i - \varphi) \le 1$ , and $a = e\cos\varphi, b = e\sin\varphi$ , the above equation can be approximated as

$$\xi_i = r_i - R - a\cos\theta_i - b\sin\theta_i \tag{4}$$

Where $\xi_i$ is the radial distance from point $L_i(x_i, y_i)$ to the base circle.

As $\sum_{i=1}^{n}\xi_i^2$ is the minimum, and $\sum_{i=1}^{n}\xi_i = 0$.

We can get:

$$R = (1/n)\sum_{i=1}^{n} r_i \tag{5}$$

$$a = (2/n)\sum_{i=1}^{n} r_i\cos\theta_i \tag{6}$$

$$b = (2/n)\sum_{i=1}^{n} r_i\sin\theta_i \tag{7}$$

It assumes that the dynamic radius of the rotary kiln is $r_i = R_c + \Delta r_i$ , where $R_c$ is the mean radius of each cross section and $\Delta r_i$ is difference value of radius of each section which can be measured by the laser sensor. And the formulas (6) and (7) can be transformed to (8) and (9):

$$a = (2/n)\sum_{i=1}^{n}\Delta r_i\cos\theta_i + (2/n)\sum_{i=1}^{n} R_c\cos\theta_i \tag{8}$$

$$b = (2/n)\sum_{i=1}^{n}\Delta r_i\sin\theta_i + (2/n)\sum_{i=1}^{n} R_c\sin\theta_i \tag{9}$$

Furthermore, formulas (8) and (9) can be change into (10) and (11):

$$a = (2/n)\sum_{i=1}^{n}\Delta r_i\cos\theta_i \tag{10}$$

$$b = (2/n)\sum_{i=1}^{n}\Delta r_i\sin\theta_i \tag{11}$$

Therefore, the geometric centre $(a,b)$ , the base circle R and the eccentricity of each section can be calculated by formulas (5), (10) and (11). By linking all the geometric centres of the measured sections, the straightness deviation of the kiln cylinder can be calculated.

## IV. EMD Methods

The Hilbert–Huang transform (HHT) was proposed by Norden E.huang in 1998, which is an effective method for analyzing the nonlinear, non-stationary signals. It mainly consists of empirical mode decomposition (EMD) and Hilbert spectral analysis [21]–[23]. As a key part of HHT, the method of EMD for decomposing signals is intuitive, direct and adaptive [21]. This decomposition method is based on local characteristic of local time domain of the signal. Based on this characteristic, any linear, stationary or nonlinear, non-stationary signal can be decomposed into a set of Intrinsic Mode Functions (IMFs) which are amplitude and frequency modulated signals. After that, Hilbert transform is used to calculate the instant amplitudes

and instant frequencies of the IMFs to form the Hilbert spectrum. The specific procedures of EMD are described as follows:

Step 1) For the given signal $x(t)$ , construct its upper envelope $u(t)$ and lower envelope $l(t)$ by connecting all local maxima and local minima with cubic spline functions. And:

$$m_{1_1} = \frac{u(t)+l(t)}{2} \tag{12}$$

Step 2) Compute the envelopes' mean $m_{1_1}$ , and $x(t)-m_{1_1}=h_1(t)$ . And the definition of IMF is proposed mainly to get the physical meaning of the instantaneous frequency. Each IMF satisfies two basic conditions [11]: (1) over the entire dataset, the number of extreme and zero crossings must either be equal or differ at most by one; (2) at any time point, the local mean value of the envelope which is defined by the average of the maximum and minimum envelopes is zero.

Step 3) If $h_1(t)$ satisfies the definition of IMF, the first-order IMF can be obtained by $IMF_1 = h_1(t)$ . And then we go to the next step. In addition, the IMF component $c_1(t)=h_{1k}(t)$ is saved. If it is not the IMF, repeat Steps 1)–3). The stop condition for the iteration is given by:

$$SD = \sum_{t=0}^{T}\left[\frac{|h_{i(j-1)}(t)-h_{ij}(t)|^2}{h_{i(j-1)}^2(t)}\right] \tag{13}$$

Where $h_{i(j-1)}(t)$ and $h_{ij}(t)$ denote the IMF candidates of the $j-1$ and $j$ iterations, respectively, and, usually, SD is set between 0.2 and 0.3.

Step 4) Separate $c_1(t)$ from $x(t)$ . Then, we could get $r_1(t)=x(t)-c_1(t)$ . $r_1(t)$ is treated as the original data. Then, repeat the above processes and the second IMF component $c_2(t)$ of $x(t)$ could be got. After repeating the process as described above for $n$ times, the n-IMFs of signal $x(t)$ could be got. Then

$$\begin{aligned} r_2(t) &= r_1(t)-c_2(t) \\ &\cdots \\ r_{(n)}(t) &= x_{(n-1)}(t)-c_{(n)}(t) \end{aligned} \tag{14}$$

Step 5) The decomposition process can be stopped when $r_{(n)}(t)$ becomes a monotonic function from which no more IMF can be extracted. By summing up Eqs. (5) and (6), we can finally obtain:

$$x(t) = \sum_{i=1}^{n} c_i(t) + r_n \tag{15}$$

Residue $r_{(n)}(t)$ is the mean trend of $x(t)$ . The IMFs $c_1(t)$ , $c_2(t)$ , . . ., $c_n(t)$ include different frequency bands ranging from high to low ones. The frequency components contained in each frequency band are different and they change with the variation of signal $x(t)$ , while $r_{(n)}(t)$ represents the central tendency of signal $x(t)$ .

After having obtained the IMFs of signal $x(t)$ by the EMD method, the Hilbert-Huang transforms of the IMFs are as:

$$\hat{c_i}(t) = \frac{1}{\pi} P\int_{-\infty}^{\infty} \frac{c_i(\tau)}{t-\tau} d\tau \tag{16}$$

Take $\hat{c_i}(t)$ as imaginary part, and $c_i(t)$ as real part, we can have an analytic signal as:

$$z_i(t) = c_i(t) + j\hat{c}_i(t) = a_i(t)e^{j\theta_j(t)} \tag{17}$$

Where

$$a_i(t) = \sqrt{c_i^2(t)+\hat{c_i}^2(t)},\ \theta_i(t) = \arctan\left(\frac{\hat{c_i}(t)}{c_i(t)}\right) \tag{18}$$

And the instantaneous frequency can be calculated by Eqs. (18) from Eqs. (19)

$$\omega_i(t) = \frac{1}{2\pi}\frac{d\theta_i(t)}{dt} \tag{19}$$

Finally, the result of Hilbert transform of each IMF component can be calculated. And the signal can be expressed as the real part (RP) by Eqs. (20)

$$x(t) = \mathrm{Re}\left(\sum_{i=1}^{n} a_i(t)e^{j\int \omega_i(t)dt}\right) \tag{20}$$

The frequency-time distribution of amplitude of each IMF component is designated as the Hilbert spectrum $H(\omega,t)$ . And the Hilbert spectrum offers the amplitude distribution from each frequency and time.

$$H(\omega,t) = \mathrm{Re}\left(\sum_{i=1}^{n} a_i(t)e^{j\int \omega_i(t)dt}\right) \tag{21}$$

## V. Experiment and Result Analysis

### A. Experiment data

As shown in part III, during the measurement, 23 sections of the rotary kiln cylinder were selected. And the laser sensor was in alignment at the rotary centre of each section. The sample frequency of the laser measurement system is 50Hz. Each cross section was measured by 3 times. We processed all the measured signals based on the geometric method and the proposed method. Fig.5 is the signals collected of Section#7 by the measured system.

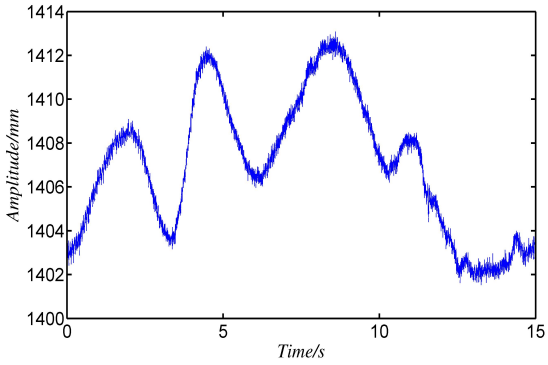


Fig.5. Original signals collected of section #7.

### B. Data processing based on geometry method

According to the geometry method mentioned in part III, we processed all the collected signals covered 23 measured sections. And the data of section 7 was taken as an example for analysis in this paper. And the processing result is

shown in Fig.6. Based on the calculation algorithm, the eccentricity $e$ of section 7 is 1.65mm. However, it can be found that this method can only provide the geometry information (eccentricity), but can not reveal the comprehensive information of the signal. In fact, there was vibration noise which affected the measurement process in the industry field.

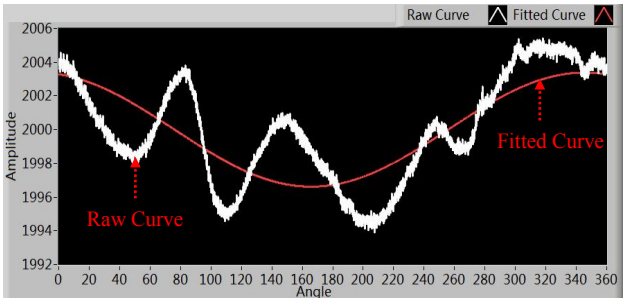


(a)

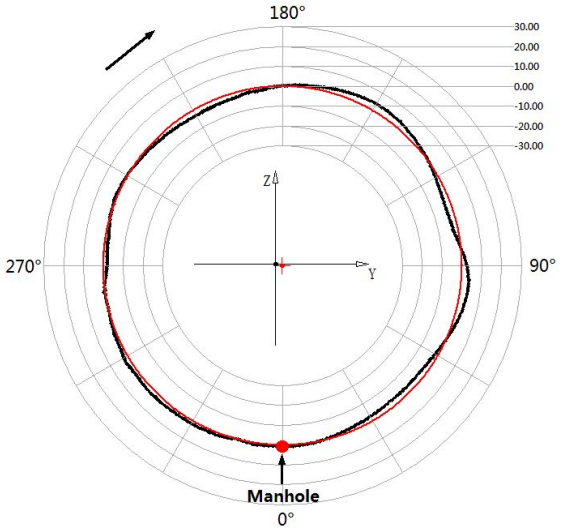


(b)

Fig.6. Measurement result for section7#. (a) The collected data and the fitted result (b) The collected data and the fitted result in the system of polar coordinates and e=1.65mm

### C. *Feature extraction based on EMD method.*

As previously pointed out, there were many shortcomings of the traditional geometry method. It is necessary to find a more appropriate method to extract the feature. Motivated by the above considerations, we proposed a new method based on the EMD algorithm. It comprises four steps, and the processing flow chart is shown in Fig.7. Firstly, the average filtering algorithm was applied in order to reduce the interference of random signal. Secondly, we used EMD to decompose signals into a serial of IMF components. Then, to select the effective IMF components, the correlation coefficient and energy coefficient were calculated. Finally, based on the spectral characteristics of the IMF components, we analyzed the physical meanings of effective IMF components. And the features can be extracted.

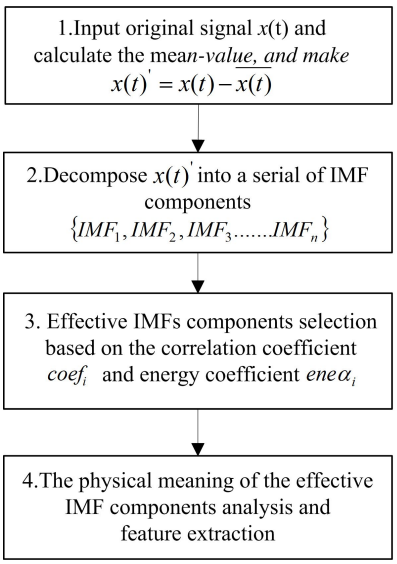


Fig.7. Feature extraction flowchart of rotary kiln cylinder profile based on EMD method

Based on the EMD method, all the signals of cross sections were processed. And the signal processed of Section #7 was shown in Fig. 8(a). The signal series is decomposed into 9 IMF components and one residue [24]. The frequencies of IMF components are arranged in an order of high to low ones. And we calculated the Hilbert spectrum of the signal, as shown in Fig. 8(b). In Hilbert spectrum, the horizontal axis represents time, vertical axis represents instantaneous frequency and the colour lines represent the amplitude. From Fig. 8(b), we can find that the energy components of the signals were mainly concentrated in low frequency bands.

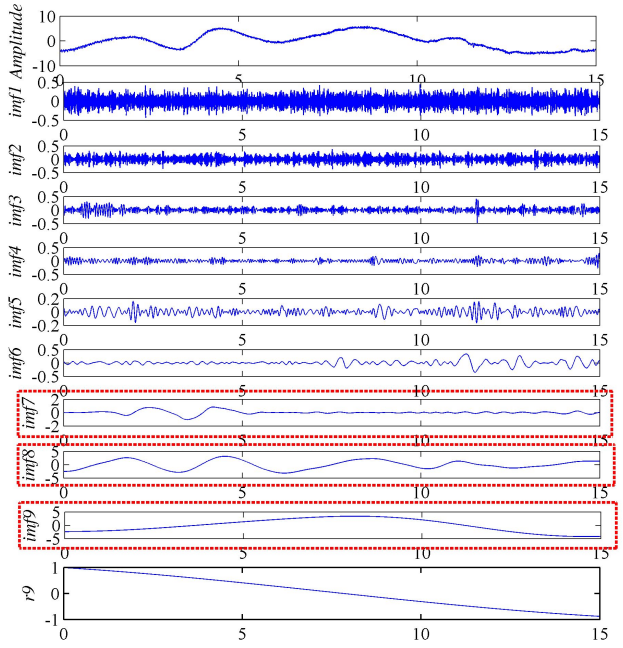


(a)

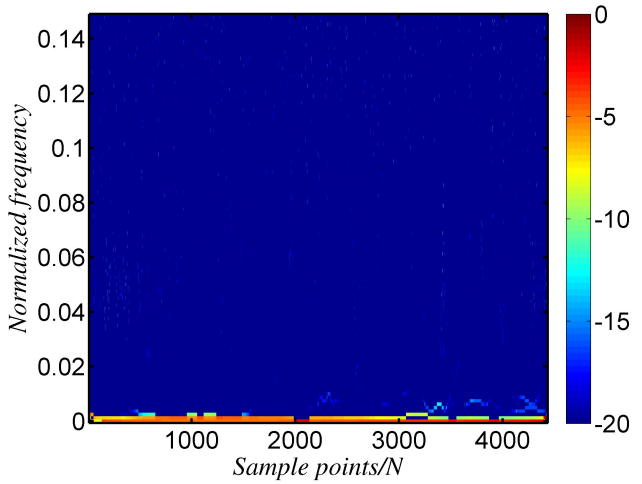


(b)

Fig. 8. (a) Data processing result based on EMD method of section #7. (b) Hilbert spectrum of the signal of section #7.

### *D. Selection of IMF components and their physical meanings.*

Based on the decomposition result of EMD method, we obtained 9 IMF components. It is necessary to filter out some IMFs as they are false components. In this research, the correlation coefficient and the energy coefficient were calculated to remove the redundant IMF components.

As IMF component is a kind of expression of approximate orthogonal method for the original signal, the real IMF components have a better correlation with the original signal [25]. The correlation coefficient between the pseudo components caused by the end effect of the syndrome and the original signal will be small. And the calculation formula is shown as (22)

$$coef_i = \frac{\sum_{t=1}^{N}(x(t)-\overline{x(t)})(c_i(t)-\overline{c_i(t)})}{\sqrt{\sum_{t=1}^{N}(x(t)-\overline{x(t)})^2}\sqrt{\sum_{t=1}^{N}(c_i(t)-\overline{c_i(t)})^2}} \quad (22)$$

Specifically, $x(t)$ is the original signal, $x_i(t)$ is the component of the ith IMF, and $coef_i$ is the relevant coefficient.

According to [26], the average energy of each IMF components can be calculated by the formula (23):

$$E_i = 1/m\left(\sum_{j=1}^{N} | a_i(t) |^2\right) \quad (23)$$

Where $m$ stands for the length of signal, and $a_i(t)$ represents the kth element of the IMF. In order to express the energy distribution of the signal of the cross sections, we define an energy coefficient of the IMF components, which can be expressed as follows:

$$E = \sum_{i=1}^{n} E_i \quad (24)$$

$$ene\alpha_i = \frac{E_i}{E} \quad (25)$$

Where $n$ is the number of the IMF components; $E$ is the summary energy of all the IMF components; $ene\alpha_i$ is the energy coefficient of the IMF $i$.

We processed the signals of three sections with the proposed method. Take the signal of section 7 as an example. It can be concluded from Table I that the correlation coefficient of IMF1~IMF6 is small while that of the IMF7~IMF9 is large. Besides, the energy of the signal is mainly concentrated at IMF7~IMF9 (over 99%). So the IMF7, IMF8 and IMF9 are picked out for further analysis.

Fig. 9 (a) showed that IMF9 component was similar to cosine signal. According to [2], when there was only straightness deviation on the cross section of the rotary kiln cylinder, the signal acquired would be sine curve or cosine curve. Moreover, Fig.9 (b) shows the frequency of IMF9 component is 0.07202HZ, which is equivalent to the rotating frequency (0.075HZ) of the rotary kiln's cylinder. Therefore, the IMF9 component was a reflection of the eccentricity of the cylinder section.

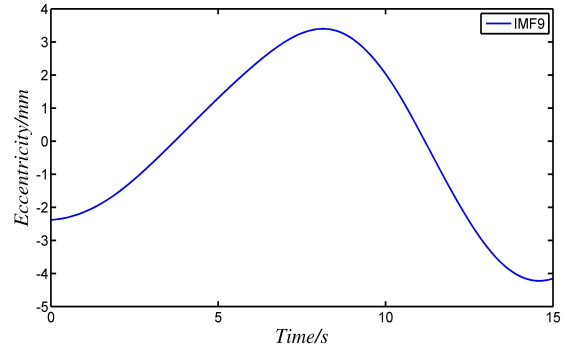


(a)

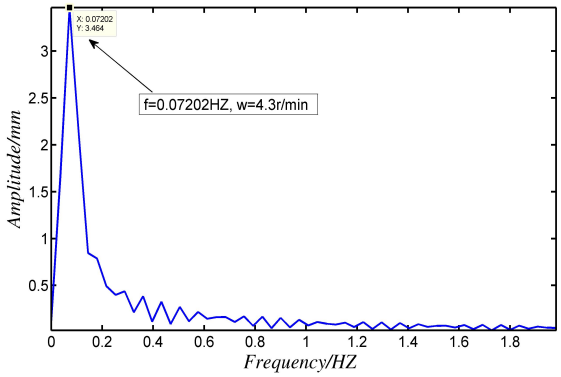


(b)

Fig.9. (a) Eccentricity separated by the proposed method (IMF9). (b) The frequency spectrum of the IMF9.

The results of onsite vibration test showed that the main frequency of low-frequency vibration was 0.18 HZ. As for IMF7, after FFT, it could be found that the frequency value of IMF7 component was about 0.185 HZ, it indicated that IMF7 represented low frequency vibration components generated in industrial field, as shown in Fig. 10 (a). Therefore, IMF8 represented surface deformation on the cylinder section, as shown in Fig. 10 (b). Based on the result, it can be found that the effective IMF components have physical meanings.

Table I Correlation coefficient and energy coefficient of each IMF component

| IMF component | IMF1 | IMF3 | IMF3 | IMF4 | IMF5 | IMF6 | IMF7 | IMF8 | IMF9 |
|---|---|---|---|---|---|---|---|---|---|
| Correlation coefficient (%) | 5.04 | 3.93 | 3.00 | 1.21 | 2.19 | 5.65 | 27.31 | 53.32 | 81.16 |
| Energy coefficient (%) | 0.29 | 0.16 | 0.08 | 0.04 | 0.02 | 0.09 | 0.92 | 30.18 | 68.22 |

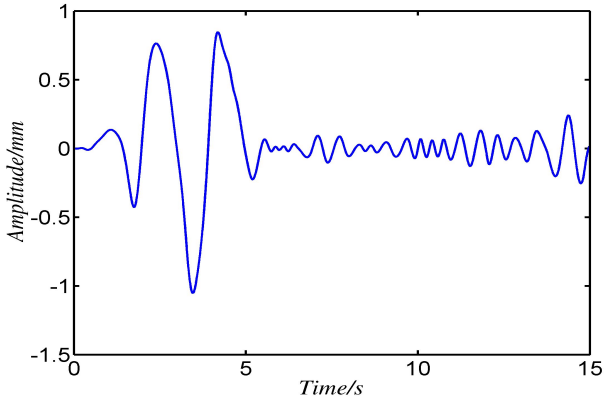


(a)

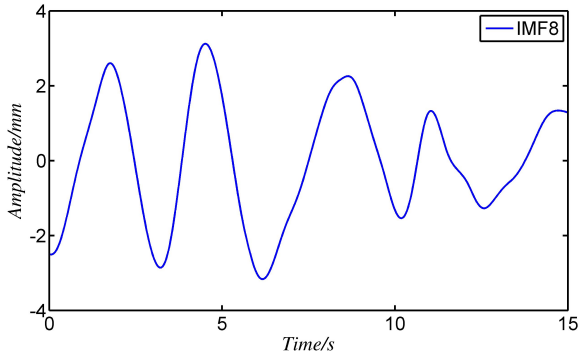


(c)

Fig.10. (a) Vibration noise separated by the proposed method (IMF7). (b) Surface deformation separated by the proposed method (IMF8)

After processing the data acquired of the 23 sections, we found that there was an IMF component (represent the eccentricity) similar to sine or cosine curve. Moreover, the correlation coefficient between this IMF component and the original signal was the maximum, which is shown in Fig. 11(a) and (b).

Also, from Fig. 11(a), we can find that the correlation coefficient between the IMF components of the straightness deviation of Sections 1-6 (head of the rotary kiln, 1st station of the rotary kiln) and Sections 20-23 (tail of the rotary kiln, 2nd station of the rotary kiln) and the original signal approached 100%, which indicated the straightness deviation at the kiln head and kiln tail was large.

The correlation coefficient between the IMF components of the straightness deviation of the middle part (Sections 7-19) and the original signal was small, while that between the IMF components of cylinder surface deformation and the original signal was large, which indicated that there was serious surface deformation in the middle part of the measured rotary kiln (2nd to 3rd stations).

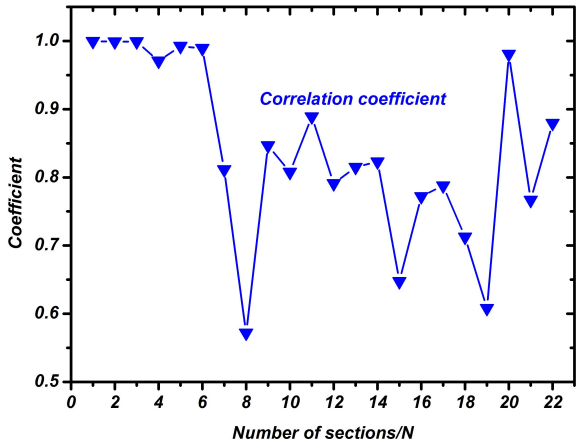


(a)

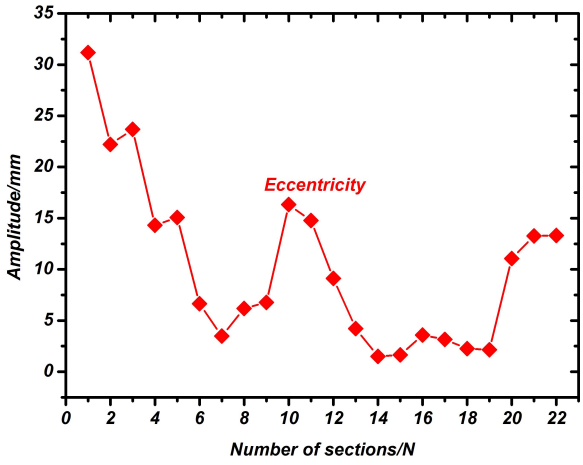


(b)

Fig.11. (a) The correlation coefficient between the IMF component of the straightness deviation and the original signals (b) Eccentricity of all measured sections based on EMD method.

### *E. Comparison with the geometry method.*

To further verify the effectiveness of EMD method, we compared the results of data processing based on the proposed method with the geometric method. As shown in Fig. 12, the eccentricity calculated with EMD method was basically the same as that calculated with geometric method. It suggested that the proposed method could be used to effectively extract the two features of straightness deviation and cylinder surface deformation. Furthermore, the proposed method could effectively separate noise signals and eliminate the effect brought by the vibration of measuring instrument.

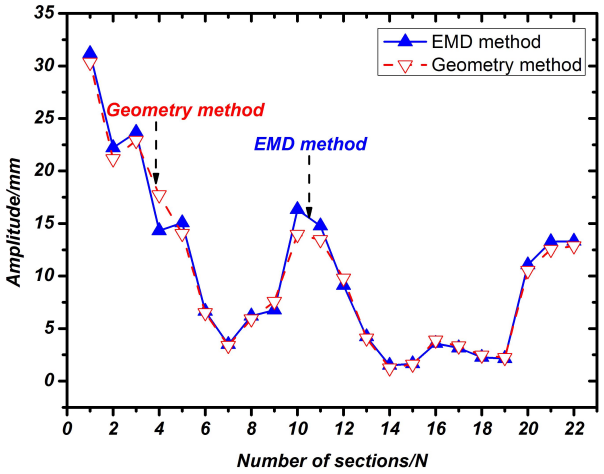


Fig.12 The straightness deviation result processed by EMD method and geometry method.

## VI. Conclusions

The straightness deviation and surface deformation of kiln cylinder are important physical parameters for evaluating the operation state of the kiln. In this paper, we made an initial investigation on the EMD-based method for feature extraction of the kiln cylinder's profile. And the main contributions and conclusions of this paper are:

(1) A feature extraction method of the rotary kiln cylinder profile was presented. We used EMD algorithm to decompose the signals into IMF components and selected the effective ones based on the correlation coefficient and energy coefficient. And the features of kiln cylinder profile can be extracted by the effective IMF components.

(2) The effective IMF components have physical meanings. Take the data of cross section#7 as an example. We can find that IMF9 represents the eccentricity; IMF8 represents the local surface deformation; IMF7 represents the on-site vibration noise.

(3) The experiments were done in the real industry field in several cement plants. The experimental results indicated that the proposed method is effective in separating the straightness deviation and the surface deformation of rotary kiln cylinder. Moreover, the proposed method can be used to process the non-stationary and non-linear signals collected and provide comprehensive information of the signals, while the traditional method can only provide the geometry information. Thus, the new method provides a viable signal processing tool for the operation state judgment of the low speed machinery like the rotary kiln.

## Acknowledgment

This research is supported and funded by National centre for rotary kiln detection technology and Hubei Digital Manufacturing Key Laboratory. We also thank the anonymous reviewers and editors for their valuable comments and suggestions.

## References

[1] Y. Zhang and Z.X. Li, "Dynamic measuring and adjustment on-line on rotary kiln", *China Building Material Equipment* 3(2002), 3–7.

[2] Y. Zhang and Zheng Weifei, "Dynamic detecting method of the axial distortion and shell distortion of rotary kiln". *CEMENT ENGINEERING* (2011)02,023

[3] X.J. Li, L.L. Jiang et al., "Research on supporting load distribution of large-scale rotary kiln with multi-support and variable-stiffness", *Chinese Journal of Computational Mechanics* 2(22) (2005), 207–213.

[4] Świtalski, Maciej. "The Measurement Of Shell's Elastic Ovality As Essential Element Of Diagnostic Of Rotary Drum's Technical State." *Diagnostyka*(2010): 37-47.

[5] Dhillon, B. S. "Multiaxial fatigue life prediction of kiln roller under axis line deflection." *Applied Mathematics and Mechanics,* Vol. 31 Issue 2, p205-214. 2010.

[6] Rusinski, Eugeniusz, Zaklina Stamboliska, and Przemysław Moczko. "Proactive control system of condition of low-speed cement machinery." *Automation in Construction,* Vol. 31, p313-324. 2013.

[7] Stamboliska, Zhaklina, Eugeniusz Rusiński, and Przemyslaw Moczko. "Condition Monitoring Techniques for Low-Speed Machines." *Proactive Condition Monitoring of Low-Speed Machines.* Springer International Publishing, 2015. 69-119.

[8] Krystowczyk, Zbigniew, and Poland Geoserverex. "Geometry Measurements of Kiln shell in Dynamic Conditions". *Cement & Building Materials* No (2004).

[9] Junsheng, Cheng, Yu Dejie, and Yang Yu. "Research on the intrinsic mode function (IMF) criterion in EMD method". *Mechanical Systems and Signal Processing,* Vol. 20 Issue 4, p817-824. 2006.

[10] Hsieh, Nan-Kai, Wei-Yen Lin, and Hong-Tsu Young. "High-Speed Spindle Fault Diagnosis with the Empirical Mode Decomposition and Multiscale Entropy Method." *Entropy,* Vol. 17 Issue 4, p2170-2183. 2015.

[11] Wu Zhaohua, Norden E. Huang, "On the filtering properties of the empirical mode decomposition", *Adv. Adaptive Data Anal.* 2 (4) (2010) 397–414.

[12] Lin, Li, and Ji Hongbing. "Signal feature extraction based on an improved EMD method." *Measurement*, Vol. 42 Issue 5, p796-803. 2009.

[13] Li, et al. "Rotational Machine Health Monitoring and Fault Detection Using EMD-Based Acoustic Emission Feature Quantification." , *IEEE Transactions on Instrumentation and Measurement* , Vol. 61 Issue 4, p990-1001. 2012.

[14] Yu, Dejie, Junsheng Cheng, and Yu Yang. "Application of EMD method and Hilbert spectrum to the fault diagnosis of roller bearings". *Mechanical systems and signal processing,* Vol. 19 Issue 2, p259-270. 2005.

[15] Nerma, Mohamed H. M., N. S. Kamel, and V. J. Jagadish. "Investigation of Using Dual Tree Complex Wavelet Transform (DT-CWT) to Improve the Performance of OFDM System." Engineering Letters, Vol. 20, no. 2, p135-142. 2012.

[16] Guo, Qiang, and Pulong Nan. "Method for feature extraction of radar full pulses based on EMD and chaos detection." *Journal of Communications & Networks* 16.1(2014):92 - 97.

[17] Xia, Chunlin, et al. "Surface characteristic profile extraction based on Hilbert–Huang transform". *Measurement*, Vol. 47, p306-313. 2014.

[18] Peng, Yonghong. "Empirical model decomposition based time-frequency analysis for the effective detection of tool breakage." J*ournal of manufacturing science and engineering,* Vol. 128 Issue 1, p154-166. 2006.

[19] Antonino-Daviu, Jose, et al. "An EMD-based invariant feature extraction algorithm for rotor bar condition monitoring." *Diagnostics for Electric Machines, Power Electronics & Drives (SDEMPED)*, 2011 IEEE International Symposium on. IEEE, 2011.

[20] Fan, Xianfeng, and Ming J. Zuo. "Machine fault feature extraction based on intrinsic mode functions." *Measurement Science and Technology* 19.4 (2008): 045105.

[21] Huang, N. E., Shen, Z., Long, S. R., Wu, M. C., Shih, H. H., Zheng, Q., ... & Liu, H. H. "The empirical mode decomposition and the Hilbert spectrum for nonlinear and non-stationary time series analysis." *In Proceedings of the Royal Society of London A: Mathematical, Physical and Engineering Sciences* .Vol. 454, No. 1971, pp. 903-995. 1998.

[22] Lu, Peng, et al. "Experimental study on flow patterns of high-pressure gas–solid flow and Hilbert–Huang transform based analysis." *Experimental Thermal and Fluid Science,* Vol. 51, p174-182. 2013.

[23] Soualhi, A., K. Medjaher, and N. Zerhouni. "Bearing Health Monitoring Based on Hilbert--Huang Transform, Support Vector Machine, and Regression." *IEEE Transactions on Instrumentation & Measurement.* Vol. 64 Issue 1, p52-62. 11p. 2015.

[24] EEMD/EMD Matlab Program and the Utilities for HHT Calculations.<http://rcada.ncu.edu.tw>.

[25] Yang, Gongliu, et al. "EMD interval thresholding denoising based on similarity measure to select relevant modes." *Signal Processing ,* Vol. 109, p95-109. 2015.

[26] Yang, Zhensheng, et al. "Application of Hilbert–Huang Transform to acoustic emission signal for burn feature extraction in surface grinding process."*Measurement,* Vol. 47, p14-21. *2014*.

Kai Zheng received a B.E. degree from Hubei University of Technology, Wuhan, China, in 2011, and a M.S. degree from Wuhan University of Technology, in 2013. He is currently a Ph.D candidate in the School of Mechanical and Electronic Engineering, Wuhan University of Technology, Wuhan, China. His research interests are wireless sensor networks, signal processing and machinery fault diagnosis.

Yun Zhang received a B.S. degree from Huazhong University of Science and Technology, Wuhan, China, in 1982. In 2004, he won the second prize of national technological innovation in China. He is currently a full-time professor in the School of Mechanical and Electronic Engineering, Wuhan University of Technology, Wuhan, China. His research interest is machinery fault diagnosis.

Chen Zhao received a B.E. degree from Wuhan University of Technology, Wuhan, China, in 2014. He is currently a graduate student of the School of Mechanical and Electronic Engineering in Wuhan University of Technology. His research interest is wireless sensor networks and machinery fault diagnosis.

Lei Liu received a B.E. degree from Wuhan University of Technology, Wuhan, China, in 2013. He is currently a graduate student of the School of Mechanical and Electronic Engineering in Wuhan University of Technology. His research interest is machinery fault diagnosis.